Deuteron NMR Measurements of Order and Mobility in the Hard Segments of a Model Polyurethane

J. A. Kornfield* and H. W. Spiess

Max-Planck-Institut für Polymerforschung, Postfach 3148, D-6500 Mainz, Federal Republic of Germany

H. Nefzger,† H. Hayen, and C. D. Eisenbach

Makromolekulare Chemie II, Universität Bayreuth, D-8580 Bayreuth, Federal Republic of Germany

Received December 18, 1990; Revised Manuscript Received March 25, 1991

ABSTRACT: Pulsed deuteron NMR results are reported for a series of segmented model polyurethanes with monodisperse hard segments containing specifically labeled sites. The hard segments consist of five piperazine rings (1–5) separated by carbonyloxytetramethyleneoxycarbonyl spacers; three labeled derivatives are used, with piperazine-d_8 at the 1,5-, 2,4-, and 3-rings. The soft segments are polydisperse poly(tetramethylene oxide) ($M_n \approx 2000$). To facilitate interpretation of the polyurethane spectra, measurements are also made on model compounds of the hard segment oligomer, and a model polymer consisting of soft segments chain extended by individual piperazine-d_8 rings. The results indicate that 85% of the hard segments exist in the hard phase, with low mobility at temperatures below 410 K ($\approx T_m - 10$ K). The rest of the hard segments appear to be dispersed in the soft phase, with high mobility at temperatures above 260 K ($\approx T_g + 60$ K). Molecular mobility is much greater at the exterior than the center of hard segments in the hard phase at temperatures between 300 and 410 K. Comparison of changes in molecular mobility and in the storage modulus with temperature (T) shows that (1) as T increases from 200 to 280 K, increase in mobility of the soft phase due to the glass-to-rubber transition and crystallite melting correlates with the 100-fold decrease in modulus in this range, (2) as T increases to 400 K, increase in mobility at the exterior of the hard phase correlates with the gradual decrease in modulus, and (3) at $T \approx 410$ K, onset of high mobility at the center of hard segments in the hard phase correlates with the loss of mechanical integrity.

1. Introduction

Microphase-separated polymers comprise a wide array of systems of practical and scientific interest: incompatible blends, diblock polymers and their blends with homopolymers, and triblock and multiblock thermoplastic elastomers. The microphase-separated structure, together with the molecular composition, controls the macroscopic properties of these systems. Standard techniques for investigating them are differential scanning calorimetry (DSC) and dynamic mechanical testing to identify transition temperatures, as well as microscopy and scattering measurements to clarify the microphase structure. Molecular motions that play an important role in determining the macroscopic mechanical properties are more difficult to assess. Fundamental observations of molecular mobility in the two phases and in the interphase of microphase-separated materials are needed to test hypotheses regarding the molecular origins of their macroscopic properties. The purpose of this investigation is to use isotopic labeling and solid-state ^{2}H NMR to obtain direct measurements of the variation of molecular motion from the core of the "hard" phase particles to the interphase between the hard and "soft" phases in a model polyurethane over a broad temperature range.

Linear polyurethane thermoplastic elastomers[1] are alternating block copolymers that exhibit rubberlike elasticity over a wide temperature range but melt at elevated temperature. Their material properties arise from the microphase separation that occurs due to segmental incompatibility between the two blocks.[2] At use temperatures, one of the phases is glassy or crystalline (hard) and the other is rubbery (soft). The extent of phase separation as well as the microphase structure has been extensively studied and is still a topic of major interest in the physics and chemistry of polyurethanes.[3-5] It is understood that the hard-phase particles serve both as multifunctional, thermoreversible cross-links and as filler particles.[6] However, little is known about the gradients in molecular mobility between the hard and soft phases. Spatially resolved measurements of molecular mobility near the interface can clarify the nature of the interphase and its role in determining the macroscopic mechanical properties of the material. In particular, such information can discriminate between hypotheses put forward to explain the softening of polyurethanes with increasing temperature: progressive dissolution of hard segments from the hard phase into the soft phase[3] or softening of the hard phase[7] or both.

To address these issues, we study a model system with monodisperse hard segments and subject to a fixed thermal treatment; spatial resolution is obtained by applying a deuterium label selectively in the hard segments, and molecular motion is observed as a function of temperature by using pulsed ^{2}H NMR. Piperazine-based polyurethanes are used in this study because the chemical stability of the hard segments makes them ideal for site-specific isotopic labeling. Pulsed ^{2}H NMR[8-10] is applied because it provides detailed information on the variation of molecular mobility in the microphases and interphase in segmented copolymers.[4,11]

Polyurethanes with piperazine-based hard segments (PIP-HSs) have been used as model systems for studies of the effect of hard and soft segment molecular weight distribution. For typical polyurethanes, containing the –NHCOO– constitutive unit, research on model poly-

* Address correspondence to this author at: Department of Chemical Engineering, California Institute of Technology, Pasadena, CA 91125.

† Present address: Bayer AG, Dormagen, Federal Republic of Germany.

0024-9297/91/2224-4787$02.50/0

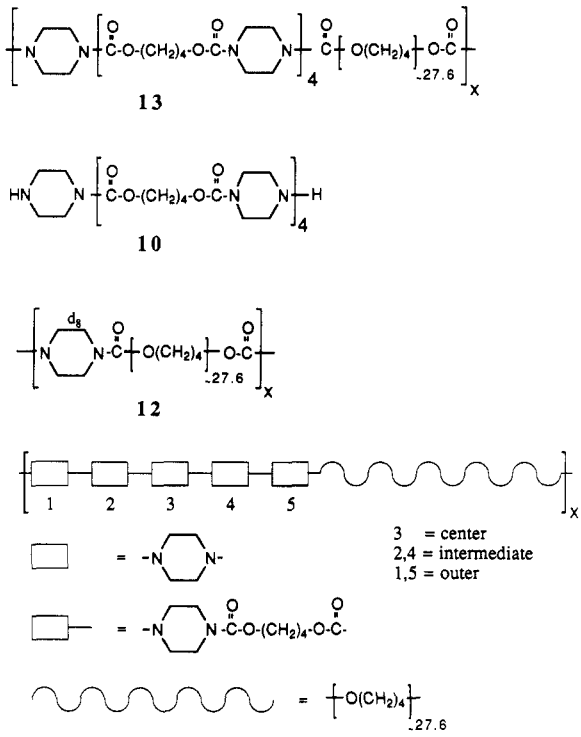

Figure 1. Chemical structure of polyurethanes and model compounds. (a) Polyurethanes consist of alternating blocks of polydisperse poly(tetramethylene oxide) soft segments, $\bar{M}_n \approx 2000$, and monodisperse piperazine/1,4-butanediol hard segments, having five 1,4-piperazinidiyl units. (b) Hard segments precursors. (c) Polymer consisting of poly(tetramethylene oxide) prepolymer chain extended with piperazine. (d) Schematic structure illustrating our nomenclature for the specific piperazine ring sites in the hard segments.

mers[12,13] is complicated by the transurethanization reaction, which destroys their tailored primary structure at temperatures that are still below the melting point of the hard phase.[13-15] Because there is no active hydrogen in the >NCOO- urethane group of PIP-HSs (see Figure 1), transurethanization does not occur, even at temperatures up to and above the melting point.[16-19] The stability of PIP-HS polyurethanes permits synthesis and comparison of model polymers with systematically varied hard segment molecular weight and molecular weight distribution. In addition, PIP-HS polyurethanes are model systems for demonstrating properties of polyurethanes that are independent of hydrogen bonding.[20]

The type of PIP-HS polyurethane we use has hard segments consisting of piperazine and carbonyloxytetramethyleneoxycarbonyl (COTMOC) spacers and soft segments of poly(tetramethylene oxide) (PTMO). These have been characterized previously using calorimetric and mechanical testing,[16-22] light scattering,[23] electron microscopy,[23] polarization microscopy,[24] and small-angle X-ray scattering (SAXS).[24] For the specific system used in this study (see Figure 1a) it has been established that chain folding does not occur in the hard segment segregated phase,[21] the long spacing of the microphase structure is 150 ± 20 Å and the q-dependence of SAXS is characteristic of microphases with sharp phase boundaries.[24] As indicated by the disappearance of scattering, the microphase separation transition temperature is approximately 430 K, only a few degrees above the melting point of the polyurethane.[24] In addition, the crystal structure of a piperazine–COTMOC hard segment model compound has been determined by wide-angle X-ray diffraction (WAXD).[25]

The following section describes the materials and the methods used for mechanical, calorimetric, and ^{2}H NMR measurements. Section 3 presents the results of these measurements. We discuss the nature of the microphases in Section 4.

2. Materials and Methods

Polyurethanes and Model Compounds. The structure of the polyurethanes used in the present study is shown in Figure 1a: the hard segments consist of exactly five piperazine rings separated by COTMOC spacers, and the soft segments are polydisperse PTMO blocks. Three labeled polyurethanes are used, differing in the location of isotopically labeled (d_8) piperazine rings in the hard segments, as shown schematically in Figure 1d: the polymer with the two outermost of the five piperazine rings deuterated is called 1,5-labeled-PEU-4, that with the two intermediate rings deuterated is 2,4-labeled-PEU-4, and that with the center ring deuterated is 3-labeled-PEU-4. As an aid in interpreting the ^{2}H NMR line shapes observed for the polyurethanes, isotopically labeled model compounds are also used: the hard segment oligomer (Figure 1b) is used as a system that can be compared to the hard microphase, and a soft segment polymer containing isolated piperazine rings (Figure 1c) may be compared to hard segments dispersed in the soft phase. The nomenclature introduced for the labeled hard segment oligomers is like that used for the polymers: the derivatives with the outermost and center piperazine rings labeled are named 1,5-labeled-diamine-4 and 3-labeled-diamine-4, respectively. The polymer with isolated labeled rings is referred to as labeled-preextended-PU.

The model elastomers with monodisperse hard segments, 13 in Figure 1, have been synthesized by using a uniform hard segment oligomer and poly(tetramethylene oxide) soft segment prepolymers with a number-average molar mass $M_n \approx 2000$ and a normal distribution of molar mass $M_w/M_n \approx 2.4$. The hard segment oligomer is α-hydro-ω-piperazinyltetrakis(1,4-piperazinediylcarbonyloxytetramethyleneoxycarbonyl), referred to as diamine-4 (10). The undeuterated, i.e., fully-protonated, hard segment diamine-4, with four repeat units and a total of five piperazine rings, was synthesized in a step-by-step synthesis starting from 1,4-butanediol, piperazine (PIP), and phosgene as described elsewhere.[22] The hard segments with selected piperazinyl units deuterated with synthesized by the same procedure, but employing piperazine-d_8 to prepare the corresponding intermediates in the sequential synthesis described in the Appendix.

Mechanical Analysis. The mechanical properties of normal PEU-4 were determined in free oscillation by using a Brabender torsion pendulum.[5,22] Samples were prepared by casting from $CHCl_3$ solution onto mercury. After the film was dry, with thickness between 0.6 and 0.8 mm, 3.5 cm × 0.5 cm strips were cut from it. Measurements were made from −130 to 180 °C with a heating rate of 1 °C/min and at a frequency of approximately 1 Hz.

Thermal Analysis. The polyurethane samples were examined by differential scanning calorimetry (DSC) between −150 and 200 °C using a Mettler DSC 30. Samples (15–18 mg) were treated by cooling from 200 to 150 °C at 10 °C/min, annealing at 150 °C for 30 min, and cooling from 150 to 50 °C at 2 °C/min and from 50 to −150 °C at 10 °C/min. The cooling rates and annealing times were chosen to minimize the time required without changing the DSC results from those of a sample slowly cooled from the melt (1 °C/min over the whole range). This slow annealing mimicks the thermal treatment used in the NMR measurements (described below). Measurements were made by using heating rates of 10, 20, and 50 °C/min.

Pulsed ^{2}H NMR. Deuteron NMR (46.07 MHz) spectra were obtained with a Bruker CXP 300 NMR spectrometer. Fully relaxed spectra were acquired with a standard quadrupolar echo sequence[8-11] $[(\pi/2)_y-\tau_1-(\pi/2)_x-D0]$ with phase cycling. Data were acquired during the $D0$ period and accumulated. The $\pi/2$ radio-frequency pulse was always less than or equal to 3.3 μs, although in some cases this resulted in flip angles somewhat less than $\pi/2$. The pulse width was limited to 3.3 μs to maintain a sufficient excitation bandwidth. The delay time, τ_1, was 30 μs, and $D0$ was chosen such that the spin–echo intensity was greater than 95%

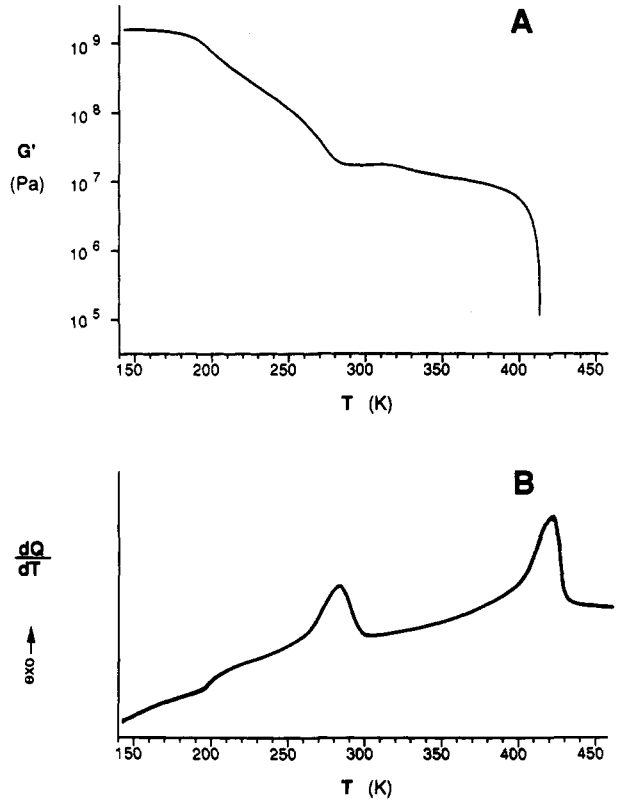

Figure 2. Macroscopic thermal and mechanical properties of the polyurethanes used in this study. (A) Dynamic shear modulus a function of temperature and (B) differential scanning calorimetry results for heat flow as a function of temperature.

of its value as $D0 \rightarrow \infty$, except at temperatures below 220 K, where the spin–lattice relaxation time increases dramatically with decreasing temperature. The spectrometer was tuned at room temperature by using D_2O; at other temperatures, only the impedance match was adjusted. Data (4096 points) were acquired at a rate of 2 MHz, shifted so that the first data point was the echo maximum, and Fourier transformed.

A Bruker B-VT 1000 unit was used to control the sample temperature over a range from 190 to 440 K. The temperature registered by the PT100 thermocouple of the Bruker unit was periodically checked against a second thermocouple and differences of up to 5 K between the readings were found to occur when operating 100 K above or below room temperature; we take ±5 K as a liberal estimate for the uncertainty in the temperature throughout the range of interest. The same temperature history was used for each sequence of measurements and consisted of warming the sample above the melting point (to 430 K) and then reducing the temperature in 5–10-K steps, allowing at least 30 min for equilibration at each step. This sequence of measurements was repeated three times for each sample.

3. Results

Mechanical Characterization. The results of torsion pendulum measurements of the dynamic modulus of PEU-4 as a function of temperature are shown in Figure 2A. Mechanical measurements were performed on the undeuterated polymer only, due to the small quantity of the labeled polyurethane synthesized. The microphase-separated structure is manifested in the monotonic decrease in the modulus with temperature, with pronounced drops correlating with established phase transitions of the pure forms of the soft and hard block materials.[17,18,22] At sufficiently low temperatures (below the glass transition of the soft segments), the storage modulus of PEU-4 is greater than 10^9 Pa; as temperature is increased from 200 to 280 K, it decreases to about 2×10^7 Pa due to the glass transition of amorphous PTMO

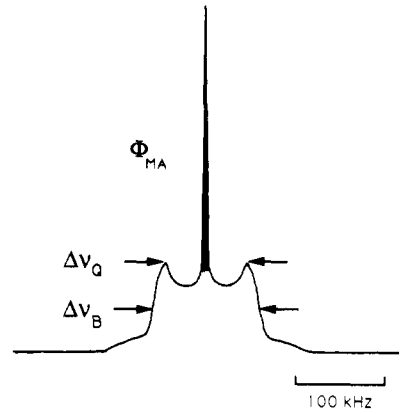

Figure 3. Line shape showing two-phase character, and definition of quantities used to characterize the spectra: the fraction of intensity due to highly motionally averaged nuclei, Φ_{MA}; the presence and separation of quadrupolar splitting peaks, $\Delta\nu_Q$; and the width at half-height of the broad line, $\Delta\nu_B$.

and the melting of crystalline PTMO. Further increase in temperature to 400 K in the plateau region lowers the storage modulus only to 5×10^6 Pa, whereas within the next 10 K the modulus drops 2 orders of magnitude as the temperature approaches the melting point of the hard phase.

Thermal Characterization. Differential scanning (DSC) calorimetry measurements were made on the undeuterated PEU-4 and all three of the labeled derivatives, and the results were found to be in good agreement with one another. The heat flow versus temperature curve observed for 1,5-labeled-PEU-4 at a heating rate of 10 °C/min is shown in Figure 2B. The glass transition of the soft phase appears as an inflection in the curve at $T_g \approx$ 196 K. A broad endotherm occurs at the melting point of crystalline PTMO, $T_{m,PTMO} \approx 281$ K, due to the semicrystalline state of the soft segments. The melting of the hard phase is evident as a similar endotherm that begins at approximately 350 K and peaks at $T_m \approx 421$ K. The peak position is somewhat lower than the value of 431 K previously reported and is about 35 K below the melting point of diethylurethane-4 (456 K).[18] The endotherm for diethylurethane-4 begins at about 420 K. Results for the hard segment oligomer[22] and preextended-PU[18] have been reported elsewhere.

Pulsed ²H NMR Results: Characteristic Features. The strength of ²H NMR as a tool for studying molecular orientation and motion in polymers arises from the coupling of the nuclear electric quadrupole moment with the electric field gradient (EFG) of the covalent bond to the deuterium. This coupling leads to a symmetric splitting of the resonant frequency of the nucleus. The magnitude of the quadrupolar splitting[8,26] is $2\omega_Q$, where

$$\omega_Q = \delta(3\cos^2\theta - 1 - \eta\sin^2\theta\cos 2\Phi)$$

and where $\delta = (3/8)(e^2Qq/\hbar)$, $e^2Qq/\hbar$ is the quadrupolar coupling constant, θ and Φ are the polar angles of the external magnetic field $\mathbf{H}_0$ in the principal axis system of the EFG, and η is the asymmetry parameter of the EFG. Typically, the bond direction is one of the principal axes of the EFG and is usually an axis of symmetry as well ($\eta = 0$).

In a static solid, the line shape gives information on the C–D bond orientation distribution. An example, relevant to the results below, is the Pake diagram[27] arising from an isotropic, rigid orientation distribution of C–D bonds (with $\eta = 0$); this line shape has characteristic singularities

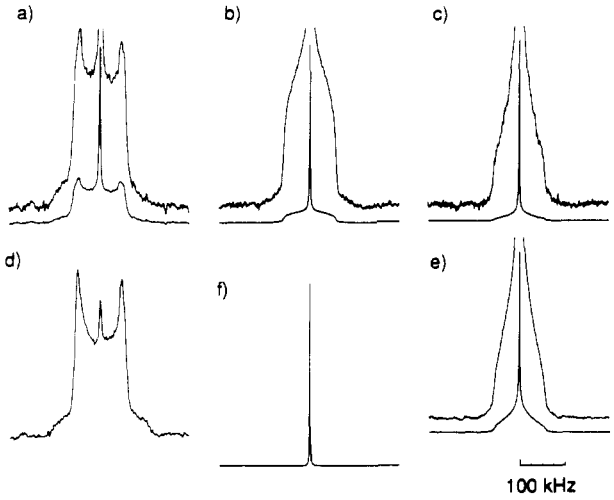

Figure 4. Broad-line deuteron NMR spectra at 360 K. (a) 3-Labeled-PEU-4, polyurethane with middle piperazine ring of the hard segments replaced with piperazine-d_8; (b) 2,4-labeled-PEU-4, polyurethane with second and fourth piperazine rings of the hard segments deuterated; (c) 1,5-labeled-PEU-4, polyurethane with outermost piperazine rings of the hard segments deuterated; (d) 3-labeled-diamine-4, hard segment precursor with middle piperazine ring deuterated; (e) 1,5-labeled-diamine-4, hard segment precursor with outermost piperazine rings deuterated; and (f) labeled-preextended-PU, soft segments chain extended with piperazine-d_8.

separated by $\Delta\nu_Q = \delta/\pi \approx 125$ kHz and feet that extend the linewidth to 250 kHz. If rapid molecular motion ($\tau \ll \delta^{-1}$) occurs in the material, reorientation of C–D bonds averages the quadrupolar splitting to varying degrees. When rapid, isotropic reorientation occurs, the quadrupolar coupling is completely averaged and the line shape collapses to a single sharp line at the center of the spectrum.

We recorded a series of 30–100 spectra for each of the six samples taken over a range of temperature. Changes in the line shape with temperature reveal the evolution of molecular motion at the labeled site. At sufficiently low temperatures, the spectra of all samples converge to a powder pattern, which differs somewhat from the Pake pattern, suggesting a slight asymmetry in the EFG ($\eta \approx 0.06$). At sufficiently high temperatures, the spectra are all completely motionally averaged. At temperatures between 280 and 390 K, the line shapes of all three labeled polyurethanes appear to be a superposition of a broad (>100 kHz) line and a much narrower line at the center of the spectrum. The broad line is indicative of a relatively rigid component. The narrow one is characteristic of a highly mobile component.

For example, at 360 K the line shapes of 3-, 2,4-, and 1,5-labeled-PEU-4 are given in Figure 4a–c. The spectra are shown both on a smaller scale based on the highest peak and on an enlarged scale based on the height of the broad signal. The broad line shape of 3-labeled-PEU-4 has the quadrupole splitting peaks and feet of the powder pattern. The broad signals of 2,4- and 1,5-labeled-PEU-4 are smoothly tapered, with width at half-height of about 110 and 75 kHz, respectively. This trend is indicative of increasing mobility with increasing distance from the center of those hard segments that are in a relatively static state. There is a strong similarity between the broad signal of 3-labeled-diamine-4 (Figure 4d) and that of 3-labeled-PEU-4 (Figure 4a) at this temperature. This is also true for 1,5-labeled-diamine-4 (Figure 4e) and 1,5-labeled-PEU-4 (Figure 4c). The spectrum of labeled-preextended-PU at 360 K (Figure 4f) is a highly averaged line at the center of the spectrum.

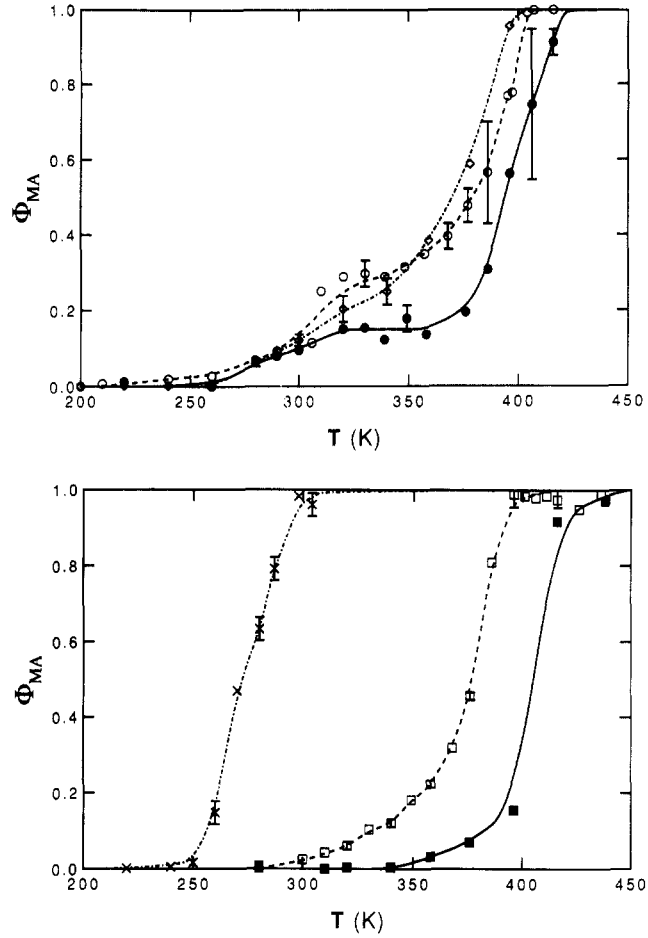

Figure 5. Temperature and position dependence of the fraction of intensity due to motionally averaged nuclei, Φ_{MA}. (a, Top) Polyurethanes labeled at the center piperazine ring, ● at the second and fourth rings, ◇, and at the outer (first and fifth) rings, ○. (b, Bottom) Model compounds: hard segment precursor labeled at the center piperazine ring, ■, and at the outer (first and fifth) rings, □; polymer containing isolated labeled rings, ×. Curves are drawn to show the trend in the data.

Temperature Dependence. To examine the variation of the line shapes of these six compounds with temperature, we compare three quantitative characteristics of the spectra that are illustrated in Figure 3: the fraction of spectral intensity in the narrow central peak, Φ_{MA}, the presence and separation of the quadrupolar splitting peaks, $\Delta\nu_Q$, and the width at half-height of the broad signal, $\Delta\nu_B$. The relative intensity of the narrow peak is computed as the integrated area from −10 to +10 kHz above the intensity at ±10 kHz, divided by the integrated area from −70 to +70 kHz. The height of the broad signal used for determination of $\Delta\nu_B$ is based on the height of the quadrupolar peaks if they are present or on the height at ±10 kHz if they are not.

The relative intensity of the narrow peak varies from zero for the powder pattern observed at sufficiently low temperature to one for the completely motionally averaged line observed at high enough temperature. In the spectra of the polyurethanes (Figure 5a), $\Phi_{MA} = 0$ for temperatures below 250 K and increases to $\Phi_{MA} \approx 0.1$ for all three in the range from 250 to 300 K. With further increase in temperature, the Φ_{MA}'s of the three spread, becoming greater for the 1,5- and 2,4-labeled-PEU-4 than for 3-labeled-PEU-4. Highly motionally averaged lines ($\Phi_{MA} = 1$) are observed for temperatures above 390 K for the 1,5- and 2,4-labeled-PEU-4 and above 405 K for 3-labeled-PEU-4. Like the polyurethanes, the spectrum of labeled-preextended-PU (in Figure 5b) has $\Phi_{MA} = 0$ for temper-

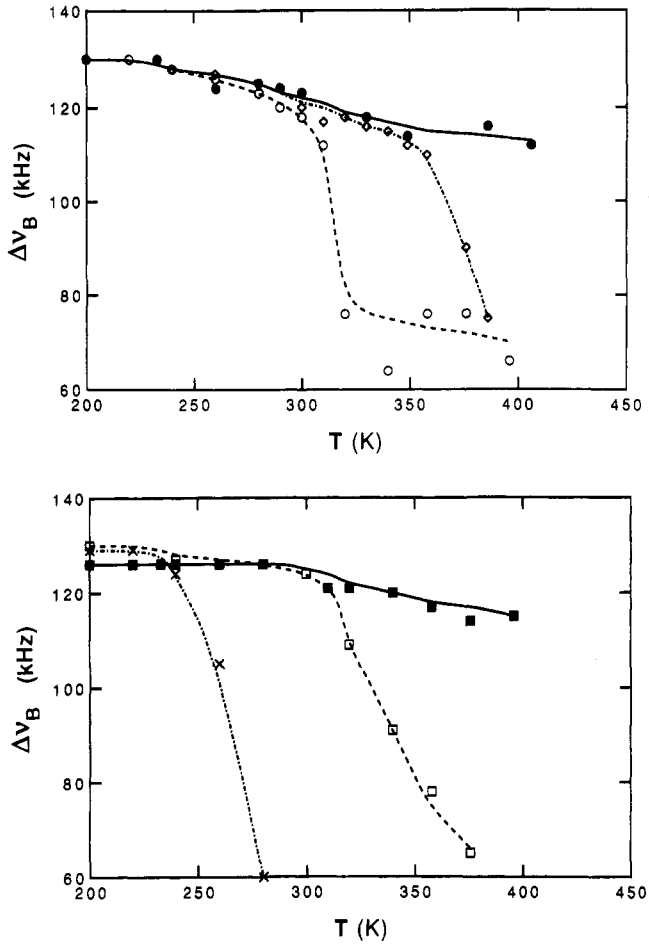

Figure 6. Width at half-height of the broad line, $\Delta\nu_B$, as a function of temperature and label position. (a, Top) Polyurethanes labeled at the center piperazine ring, ●, at the second and fourth rings, ◇, and at the outer (first and fifth) rings, ○. (b, Bottom) Model compounds: hard segment precursor labeled at the center piperazine ring, ■, and at the outer (first and fifth) rings, □; polymer containing isolated labeled rings, ×.

atures below 250 K. Between 250 and 300 K it increases steadily to $\Phi_{MA} = 1$. The $\Phi_{MA}(T)$'s of both 1,5- and 3-labeled-diamine-4 have similar sigmoidal shapes. The $\Phi_{MA}(T)$ for the center piperazine of diamine-4 appears at about 30 K higher temperature than for the outermost piperazines.

The width at half-height of the broad signal, $\Delta\nu_B$, is an indicator of the degree of partial motional averaging in the relatively rigid component. It has a maximum value of about 130 kHz for the undistorted powder pattern, which decreases with motional averaging. For the polyurethanes, $\Delta\nu_B$ decreases slightly over the range from 200 to 300 K (Figure 6a). At higher temperatures, the width of the broad signal decreases most rapidly for the end-most piperazine rings and most gradually for the center position. For 3-labeled-PEU-4, $\Delta\nu_B$ remains greater than 100 kHz up to 405 K, above which the broad signal disappears. The results for the hard segment oligomers, shown in Figure 6b, are again similar to those for the corresponding polyurethanes: the width of the broad signal decreases only slightly for temperatures up to 300 K, above which $\Delta\nu_B$ decreases strongly for the end-labeled sites and gradually for the center-labeled site. Isolated, labeled piperazine rings in a soft segment polymer show a rapid decrease in the width of the broad signal over the range from 250 to 280 K (Figure 6b).

The presence of quadrupolar splitting peaks in these spectra is indicative of a highly rigid state. The undistorted powder pattern has $\Delta\nu_Q \approx 115$ kHz. With increasing temperature, partial motional averaging decreases the splitting between the quadrupolar peaks and eventually leads to their disappearance. For the three polyurethanes there is little change in the quadrupolar splitting up to 280 K. As the temperature increases to 300 K, the quadrupolar splitting peaks disappear from the spectra of the end and intermediate piperazine sites. However, these peaks remain in the spectrum of the center piperazine ring up to 405 K, although $\Delta\nu_Q$ decreases for temperature above 300 K (Figure 7). The two hard segment oligomers, labeled at the outer and at the center piperazine rings, show no change in $\Delta\nu_Q$ up to 280 K, followed by the disappearance of quadrupolar peaks for the end-labeled oligomer and a steady decrease in the splitting for the center-labeled oligomer. For the center piperazine ring of the hard segment, $\Delta\nu_Q(T)$ is almost identical for the polyurethane and oligomer (Figure 7). The labeled-pre-extended-PU spectrum shows some distortion of the separation between the quadrupolar peaks at 240 K, and these peaks are already gone from its spectrum at 260 K.

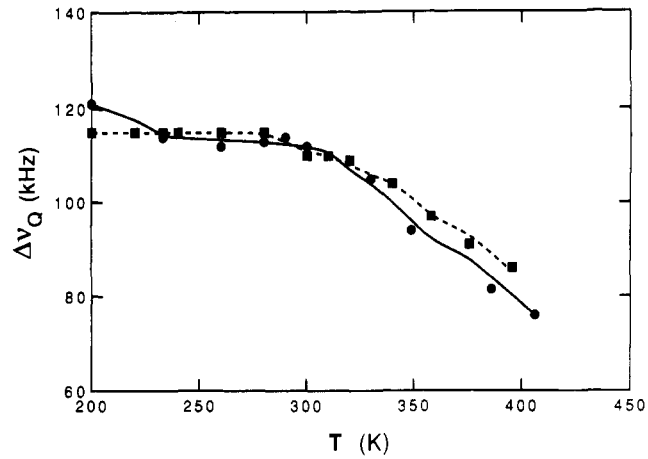

Figure 7. Separation of quadrupolar splitting peaks, $\Delta\nu_Q$, as a function of temperature and label position for the polyurethane labeled at the center piperazine ring, ●, and for the hard segment precursor labeled at the center piperazine ring, ■.

4. Discussion

The deuteron NMR spectra of the labeled polyurethanes slowly cooled from the melt show two qualitatively distinct motional states over the temperature range from 260 to 400 K (e.g., at 360 K, as shown in Figure 4). Although the precise nature of the motion in these systems is not sufficiently well characterized to allow us to simulate the observed line shapes, certain general characteristics of the motion can be inferred from them. The nuclei contributing to the broad line must be on carbon–deuterium bonds with restricted mobility, because line shapes that have a tapered appearance due to partial motional averaging, but remain >100 kHz wide, are characteristic of a rapid (>10^7-Hz rate), large amplitude (>±30°) libration *about a rigid axis*.[28] On the other hand, the nuclei contributing to the narrow (<10-kHz width) line are largely motionally averaged due to rapid molecular motions that essentially explore all orientations or that produce a nearly tetrahedral jump angle for C–D bonds or show a combination of such motions.[34] By comparing the two components of the polyurethane spectra to the spectra of the model compounds, we can infer the relationship of the microphases in the polyurethane to those represented in the model compounds.

Partitioning of the Hard Segments between the Hard and Soft Phases. The motionally averaged peak

appears in the spectra of all of the polyurethanes at the same temperature as it does for isolated piperazine rings in a chain-extended soft segment polymer (see Figure 5). Over the temperature range from 250 to 300 K, where the line shape of labeled-preextended-PU changes from a static powder pattern to a motionally averaged peak, the narrow peaks in the spectra of the three labeled polyurethanes all have the same relative intensity and increase to $\Phi_{MA} \approx 0.1$ at 300 K. The polymer with isolated piperazine groups does not phase separate, and the motion of the labeled rings in it provides a reasonable model for the motion of a hard segment completely surrounded by the soft phase. Therefore, the observed behavior in the different labeled sites in the polyurethanes is consistent with assigning the narrow peak in their spectra between 260 and 300 K to hard segments that are homogeneously dispersed in the soft phase. This interpretation of the initial rise in Φ_{MA} for the spectra of 1,5-, 2,4-, and 3-labeled-PEU-4 is based on the behavior of Φ_{MA} for labeled-preextended-PU, independent of the explanation for the onset of motion in the soft phase.

Subsequent measurements on PEU-4 with perdeuterated soft segments show that a narrow peak appears at 220 K and the spectrum collapses to a single narrow line at 290 K.[29] This is very similar to the behavior observed for labeled-preextended-PU, but shifted to ~10 K lower temperature. Together with the DSC measurements that show T_g = 196 K and T_m = 281 K for the semicrystalline soft phase, the progressive motional averaging of PTMO or piperazine segments in the soft phase from 220 to 300 K can be attributed to both the glass transition and crystallite melting. Because one-dimensional ^2H NMR line shapes are averaged by motions with rates above 10^6 Hz, the glass transition is manifested in Φ_{MA} at 50–60 K above T_g as determined by DSC, which is sensitive to motions slower than about 0.1 Hz;[30,31] the magnitude of this temperature shift is in accord with the WLF equation. Thus, both the dynamic glass transition (at ~250 K) and the soft segment melting occur in the range where Φ_{MA} of labeled-preextended-PU increases from 0 to 1.

There is a plateau in Φ_{MA} of the center-labeled polyurethane from 310 to 350 K (Figure 5a) that allows us to determine the degree of phase separation. This temperature range lies somewhat above the transition to complete motional averaging of piperazine groups in the soft phase and somewhat below the onset of significant motional averaging of the center piperazine of the crystalline hard segment oligomer. If we take these two states as representative of the soft and hard phases in the polyurethane, then we expect the nuclei in both of the corresponding motional states to be quantitatively represented in the spectra in this temperature range.[32] Thus, the value of Φ_{MA} for the center-labeled polyurethane in this plateau, $\Phi_{MA} = 0.15 \pm 0.02$, is equal to the fraction of hard segments dispersed in the soft phase. This value is consistent with an estimate of $\Phi = 0.15 \pm 0.07$, based on measurements of the glass transition temperature T_g of the soft phase and the assumption that an increase in T_g due to dispersion of hard segments in the soft phase follows a linear blending law.[18]

Composition and Organization of the Hard Phase. The broad line shapes of the respectively labeled polyurethanes and oligomers are surprisingly similar. The increase in Φ_{MA} in the hard segment oligomers first for 1,5-labeled-diamine-4 and last for 3-labeled-diamine-4 is very much like its increase in the hard segments in the polyurethanes first for 1,5-labeled-PEU-4 and last for 3-labeled-PEU-4 in the range from 300 to 410 K (Figure 5). The variation of $\Delta\nu_B$ with temperature at the 1,5- and 3-sites is nearly the same for both the polyurethane and the oligomer (Figure 6). The $\Delta\nu_Q$'s of the 1,5-labeled hard segment polyurethane and oligomer are both relatively constant up to about 280 K, above which the quadrupolar peaks disappear from both spectra. The 3-labeled hard segment polyurethane and oligomer have almost identical $\Delta\nu_Q(T)$ (Figure 7).

The strong similarity between the broad line shapes of the polyurethane and the oligomer for hard segments labeled at the outermost and center piperazine ring(s) suggests that the hard phase of the multiblock copolymer and the crystalline hard segment oligomer are very similar on the local scale that controls molecular motion of the piperazine rings. We believe this indicates that the hard domains in the PEU-4 are pure and organized with a degree of order similar to that of the crystalline oligomer diamine-4. Well-organized packing of hard segments in the microphase structure of PEU-4 is consistent with DSC results that show the enthalpy of melting of the hard phase increases nearly linearly with hard segment length up to four repeat units[22] and with SAXS results that suggest the phase boundaries are sharp.[24] Although we cannot rule out some disorder in both the hard microphase and crystalline diamine-4,[33] it is remarkable that the constraints imposed by the soft segments do not produce a significant increase in packing defects in the hard phase of PEU-4 relative to the hard segment model compound.

A gradient of mobility from the center to the exterior of the hard segments is evident in both the model oligomers and the relatively rigid phase of PEU-4 between 300 and 410 K (Figures 4–6). Separate experiments on EUE-4 (a triblock of PTMO–diamine-4–PTMO)[34] and on diamine-2 (model oligomer with three piperazine rings)[35] show similar gradients of molecular mobility. In PEU-4 and EUE-4, microphase separation aligns exterior groups of the segregated hard segments at the interface between the hard and soft phases. WAXD results suggest that hard segment oligomers crystallize with exterior amines aligned in a plane.[25] If the crystalline hard segments in both the polymers and oligomers do assume a stacked arrangement, then the mobility gradient may be explained by greater motional freedom at the interface than at the interior. We do not have sufficient WAXD results on diamine-4 to confirm this view.

Direct evidence of a gradient in mobility among structurally similar, even identical, moieties is quite interesting. Progressive increase in mobility with temperature first near the interface and then near the interior of the hard microphase has been suggested previously[36] but not directly observed. (In contrast, rapid molecular motion in polymers below the melting point is well documented;[8] and differences in mobility of structurally distinct moieties within a polymer crystal have been characterized.[28])

Relation to Macroscopic Mechanical Properties. One of the goals of this research is to clarify the role of molecular motion in determining the macroscopic properties of polyurethanes. Therefore it is interesting to consider the correlation between changes in molecular motion and in the storage modulus as functions of temperature. At temperatures below 200 K, the storage modulus of PEU-4 at approximately 1-Hz strain frequency is greater than 10^9 Pa; as the temperature is increased to 280 K, it decreases gradually to about 2×10^7 Pa as amorphous PTMO soft segments move from the glassy to rubbery state and crystalline PTMO soft segments melt. This correlates with the observation of the onset of motion in those hard segments that are dispersed in the soft phase.

We note again that the glass-to-rubber transition observed mechanically at 1 Hz is manifested in averaging of the ²H NMR spectrum at $\sim 10^7$ Hz at 50–60 K higher temperature.

In the plateau region (280–400 K), the ²H NMR results suggest that the increase in molecular mobility at the outer piperazine rings of hard segments in segregated domains gives rise to the gradual decrease in G' to 5×10^6 Pa; but in this region the center piperazine rings are still fixed, consistent with the fact that the hard segments still act as cross-links. Increase in molecular mobility at the interface between the hard and soft phase in the plateau region suggests that the decrease in modulus on this temperature range is due to a softening of the effective filler particles provided by the hard phase. No evidence of dissolution of hard segments with increasing temperature is found in this range; this observation, although not definitive, suggests that softening of PEU-4 between 280 and 400 K is not due to a decrease in the degree of phase separation. Above 400 K the fraction of highly mobile piperazine rings at the center of the hard segments rises dramatically from 50 to 100% over a 10-K range, correlating with the total loss of elastomeric properties as determined by the dynamic mechanical spectrum.

Comparison to Other NMR Studies. The distinctive feature of this approach relative to previous NMR studies of segmented thermoplastic elastomers is the site-specific nature of the information obtained. Previous studies have been made using pulsed ²H NMR to study motion of hard segments as opposed to soft segments of a polyurethane by labeling the flexible spacers throughout the hard segment.[4] Elegant applications of multitechnique solid-state ¹³C NMR have characterized the molecular mobility at each chemically distinct carbon in a family of segmented thermoplastic elastomers,[37] but again spatial resolution of segments was not possible on that basis. Similarly, early investigations using pulsed ¹H NMR revealed evidence of motional gradients between and within the hard and soft microphases of polyurethanes[38] but could not provide site specific information on either phase. The use of ²H NMR applied to isotopically labeled model polymers and model compounds provides site selectivity. This approach is particularly well suited for investigation of molecular mobility in and near the interphase region, which is particularly difficult to characterize.

Acknowledgment. Support for this research was provided by the U.S. National Science Foundation through the NATO Postdoctoral Fellowship Program (supporting J. Kornfield) and by the Bundesminister für Forschung und Technologie (supporting H. Hayen, Grant No. 03EiBay 5). We appreciate the many fruitful discussions of this research with D. Meltzer, T. Pakula, and G. Planer.

Appendix: Synthesis of Polyurethanes and Model Compounds

The synthesis and characterization of the key deuterium-labeled intermediates, the hard segment oligomers, and the model polymers are described below, following Schemes I–III. The numbers of the compounds are used to refer to the normal, fully protonated compounds; the compound number with a suffix d_8 is used for labeled intermediates containing a single piperazine ring to designate that the ring is deuterated, and a letter suffix is used for labeled compounds with distinguishable piperazine rings to designate which of the rings is/are labeled.

The architecture of the hard segments is controlled by capping one of the functional groups of each difunctional intermediate, using *tert*-butyl and carbobenzoxy (CBO) protecting groups for the OH and NH groups of BDO and PIP, respectively, as shown in Scheme I.

Scheme I
Synthesis of Singly Protected Repeat Units, Key Intermediates in the Synthesis of Monodisperse, Selectively Labeled Hard Segments and Their Model Compounds[a]

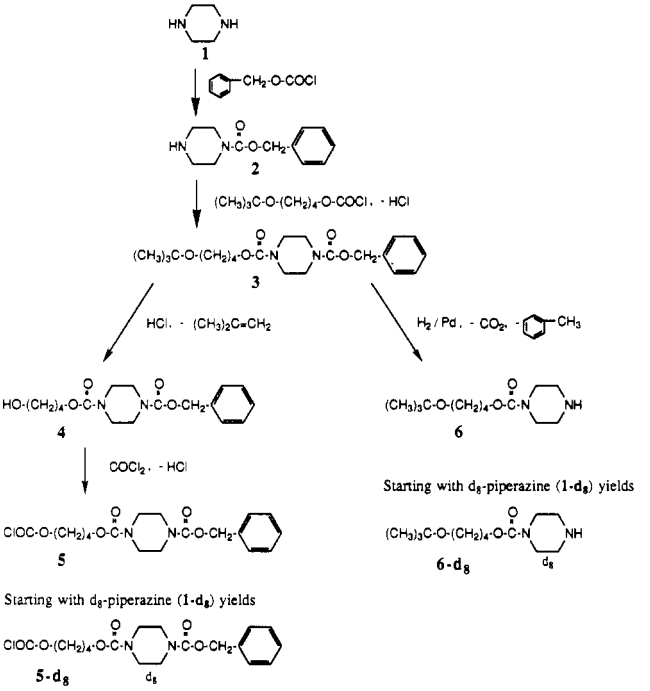

[a] See Scheme II. Compound 5 (or 5-d_8) has an active chloroformate and a carbobenzoxy- (CBO) protected NH; compound 6 (or 6-d_8) has an active secondary amino group and a *tert*-butyl-protected OH.

Benzyl piperazinecarboxylate-d_8 (2-d_8) was obtained by condensation of 50 mmol of piperazine-d_8 dihydrochloride (dissolved in methanol/water) with 25 mmol of benzyl chloroformate (Fa. Fluka) at pH 3.5; the reaction product was extracted with toluene and distilled. Bp = 135 °C (0.2 mbar); yield 71%; IR (film) 3320 (NH), 2280–2060 (CD), 1690 cm^{-1} (C=O); ¹H NMR ($CDCl_3$) δ 1.60 (s, NH, 1 H), 5.10 (s, CH_2O, 2 H), 7.32 (s, C_6H_5, 5 H).

Benzyl 4-(*tert*-butyloxy)butyl piperazine-d_8-1,4-dicarboxylate (3-d_8) was obtained by reacting 1,4-butanediol monochloroformate with 2-d_8 in a 1:1 mole ratio in a stirred $CHCl_3$ solution, with 1 M Na_2CO_3 solution as HCl scavenger. The yield after subsequent extraction of the organic phase with 2 N aqueous HCl, 5% $NaHCO_3$, and H_2O and evaporation of $CHCl_3$ was 75%. IR (film) 2280–2060 (CD), 1690 cm^{-1} (C=O); ¹H NMR ($CDCl_3$) δ 1.20 (s, $C(CH_3)_3$, 9 H), 1.65 (m, $CH_2CH_2CH_2$, 4 H), 3.30 (t, CH_2O, 2 H), 4.06 (t, $COCH_2$, 2 H), 5.1 (s, $OCH_2C_6H_5$, 2 H), 7.32 (s, C_6H_5, 5 H).

Benzyl 4-(Chloroformyloxy)butyl Piperazine-d_8-1,4-dicarboxylate (5-d_8). Cleavage of the *tert*-butyl group in 3-d_8 with 4 N HCl and subsequent phosgenation of the hydroxyl group gave the chloroformate 5-d_8 in 90% yield. IR (film) 2280–2060 (CD), 1700 (C=O, chloroformyl), 1690 cm^{-1} (C=O); ¹H NMR ($CDCl_3$) δ 1.63 (m, $CH_2CH_2CH_2$, 4 H), 4.15 (t, $CH_2CH_2C(=O)$, 2 H), 4.35 (t, $CH_2OC(=O)Cl$, 2 H), 5.1 (s, $OCH_2C_6H_5$, 2 H), 7.32 (s, C_6H_5, 5 H).

4-(*tert*-Butyloxy)butyl Piperazine-d_8-4-carboxylate (6-d_8). The CBO group in 3-d_8 was removed by 4 h of hydrogenation at 10 bar of H_2 pressure at 55 °C in the presence of Pd/C to give the secondary amine 6-d_8. Yield, 50%; IR (film) 3320 (NH), 2280–2060 (CD), 1690 cm^{-1} (C=O); ¹H NMR ($CDCl_3$) δ 1.18 (s, $C(CH_3)_3$, 9 H), 1.63 (m, $CH_2CH_2CH_2$, 4 H), 1.82 (s, NH, 1 H), 3.43 (t, CH_2O, 2 H), 4.08 (t, $CH_2CH_2C(=O)$, 2 H).

Benzyl 4-*tert*-Butoxybutyl 1,1′-[1,4-Butanediylbis(oxycarbonyl)]bis(piperazine-4-carboxylate), Deuterated at Ring a (7a) and Deuterated at Ring b (7b). 7a was prepared by reacting 5-d_8 with 6, and 7b was obtained by reacting 5 with 6-d_8

Scheme II
Synthesis of Monodisperse Hard Segment Model Compounds with Four Repeat Units (10, Diamine-4) and Its Selectively Deuterated Derivatives[a]

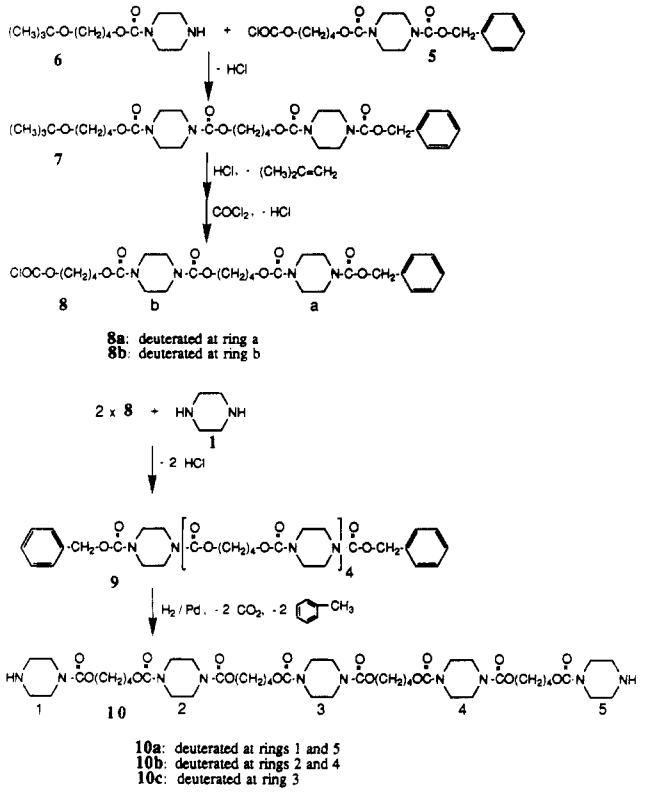

[a] **10a**, 1,5-labeled-diamine-4, from **8a** (8 deuterated at ring a) and **1**; **10b**, 2,4-labeled-diamine-4, from **8b** (8 deuterated at ring b) and **1**; and **10c**, 3-labeled-diamine-4, from **8** and **1**-d_8.

Scheme III
Synthesis of Chain-Extended Soft Segment Polymer with Isolated Piperazine-d_8 Rings, 12, and Segmented Polyurethanes with Monodisperse, Selectively Deuterated Hard Segments, 13[a]

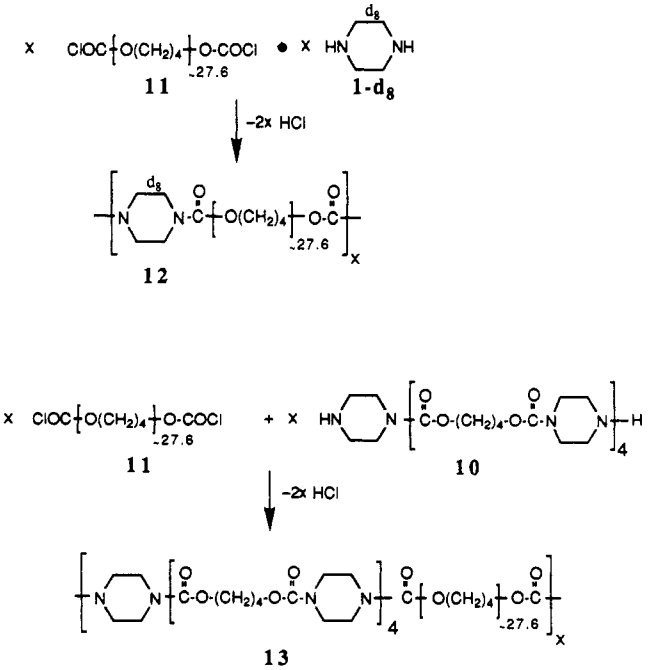

[a] **13a**, 1,5-labeled-PEU-4; **13b**, 2,4-labeled-PEU-4; and **13c**, 3-labeled-PEU-4.

under the same conditions as for the fully protonated species (see ref 29) (Scheme II). Yield, 70–75%; IR (KBr) 2280–2060 (CD), 1690 cm^{-1} (C=O); ^{1}H NMR ($CDCl_3$) δ 1.18 (s, $C(CH_3)_3$, 9 H), 1.63 (m, $CH_2CH_2CH_2$, 8 H), 3.35 (t, CH_2O^tBu, 2 H), 3.42 (s, NCH_2, 8 H), 4.10 (m, $CH_2OC(=O)$, 6 H), 5.12 (s, $OCH_2C_6H_5$, 2 H), 7.32 (s, C_6H_5, 5 H).

Benzyl 4-(Chloroformyl)butyl 1,1′-[1,4-Butanediylbis(oxycarbonyl)]bis(piperazine-4-carboxylate), Deuterated at Ring a (8a) and Deuterated at Ring b (8b). **8a** and **8b** were obtained by further reacting **7a** and **7b**, respectively, as shown in reaction Scheme II (under conditions analogous to the synthesis of **5** from **3** in Scheme I). Yield, 95%; IR (KBr) 2280–2060 (CD), 1770 (C=O, chloroformyl), 1690 cm^{-1} (C=O); ^{1}H NMR ($CDCl_3$) δ 1.63 (m, $CH_2CH_2CH_2$, 8 H), 3.45 (s, NCH_2, 8 H), 4.12 (t, $CH_2OC(=O)$, 6 H), 4.35 (t, $CH_2OC(=O)Cl$, 2 H), 5.12 (s, $OCH_2C_6H_5$, 2 H), 7.32 (s, C_6H_5, 5 H).

Dibenzyl Urethanes (9a–c). Dibenzyl urethane **9a**, with labeled rings at positions 1 and 5 (cf. **10** in Scheme II), was obtained by condensation of **8a** with piperazine (**1**); **9b**, deuterated at rings 2 and 4, was synthesized from **8b** and **1**. Condensation of unlabeled **8** with piperazine-d_8 (**1**-d_8) gave **9c**. Yield, 80–85%; IR (KBr) 2280–2060 (CD), 1770 (C=O, chloroformyl), 1690 cm^{-1} (C=O); ^{1}H NMR ($CDCl_3$) δ 1.65 (m, $CH_2CH_2CH_2$, 16 H), 3.35 (s, $>NCH_2-$, 24 H or 32 H), 4.14 (m, $CH_2OC(=O)$, 16 H), 4.35 (t, $CH_2OC(=O)Cl$, 2 H), 5.12 (s, $OCH_2C_6H_5$, 4 H), 7.32 (s, C_6H_5, 10 H).

Labeled Diamine-4 (10a–c). 1,5-Labeled diamine-4 (**10a**) was synthesized from **9a** by hydrogenation under reaction conditions analogous to the synthesis of **6** from **3**; 2,4- and 3-labeled-diamine-4, **10b** and **10c**, were obtained in a similar procedure by starting from **9b** and **9c**, respectively. Yield, 70–85%; IR (KBr) 2280–2060 (CD), 1690 cm^{-1} (C=O). ^{1}H NMR ($CDCl_3$) of 1,5-labeled-diamine-4: δ 1.63 (m, $CH_2CH_2CH_2$, 16 H), 1.83 (s, NH, 2 H), 3.37 (s, $>NCH_2-$, 24 H), 4.08 (m, $CH_2OC(=O)$, 16 H). ^{1}H NMR ($CDCl_3$) of 2,4-labeled-diamine-4: δ 1.63 (m, $CH_2CH_2CH_2$, 16 H), 1.83 (s, NH, 2 H), 2.80 (t, CH_2NH, 8 H), 3.37 (s, $>NCH_2-$, 16 H), 4.08 (m, $CH_2OC(=O)$, 16 H). ^{1}H NMR ($CDCl_3$) of 3-labeled-diamine-4: δ 1.63 (m, $CH_2CH_2CH_2$, 16 H), 1.83 (s, NH, 2 H), 2.80 (t, CH_2NH, 8 H), 3.37 (s, $>NCH_2-$, 24 H), 4.08 (m, $CH_2OC(=O)$, 16 H).

Labeled-Preextended-PU (12) was synthesized by using the same procedure described in ref 22 for the fully protonated preextended-PU, by condensation of the bischloroformate of PTMO (**11**) and piperazine-d_8 (**1**-d_8) (Scheme III).

Labeled PEU-4 (13a–c). The specifically labeled segmented polyurethane elastomers were synthesized by a condensation reaction between the bischloroformate of PTMO (**11**) and the corresponding labeled diamine-4 (**10a**, **10b**, or **10c**). The reaction conditions were similar to those described for the fully protonated elastomers.[22] Number-average and weight-average molar masses, M_n and M_w, were determined by gel permeation chromatography in $CHCl_3$, based on calibration with polystyrene standards (Waters Ultrastyragel columns 10^3, 10^4, and 10^5 Å). **1,5-Labeled-PEU-4 (13-a)**: M_n = 15 500; M_w = 34 000; ^{1}H NMR ($CDCl_3$) δ 1.53 (m, OCH_2CH_2 from PTMO), 1.72 (m, OCH_2CH_2 from COTMOC), 3.41 (m, OCH_2CH_2 from PTMO), 3.45 (s, $>NCH_2-$), 4.04 (m, $CH_2OC(=O)$; ^{13}C NMR ($CDCl_3$) δ 25.6 (OCH_2CH_2 from COTMOC), 26.5 (OCH_2CH_2 from PTMO), 43.5 ($>NCH_2-$), 65.1 (OCH_2 from COTMOC), 70.5 (OCH_2 from PTMO), 155.2 (C=O). **2,4-Labeled-PEU-4 (13a)**: M_n = 51 000; M_w = 73 000. **3-Labeled-PEU-4 (13a)**: M_n = 40 000; M_w = 50 000.

References and Notes

(1) Saunders, J. H.; Frisch, K. C. *Polyurethanes: Chemistry and Technology*; Wiley Interscience: New York, 1962.
(2) Copper, S. L.; Tobolsky, A. V. *J. Appl. Polym. Sci.* **1966**, *10*, 1837.
(3) Koberstein, J. T.; Russell, T. P. *Macromolecules* **1986**, *19*, 714.
(4) Dumais, J. J.; Jelinski, L. W.; Leung, L. M.; Gancarz, I.; Galambos, A.; Koberstein, J. T. *Macromolecules* **1985**, *18*, 116.
(5) Camarago, R. E.; Macosko, C. W.; Tirrell, M.; Wellinghoff, S. T. *Polymer* **1985**, *26*, 1145.
(6) Oertel, H. *Bayer Farben Rev.* **1965**, *11*, 1. Estes, G. M.; Seymour, R. W.; Cooper, S. L. *Macromolecules* **1971**, *4*, 452.
(7) Estes, G. M.; Huh, D. S.; Cooper, S. L. In *Block Polymers*; Aggarwall, S. L., Ed.; Plenum Press: New York, 1970. Seymour, R. W.; Estes, G. M.; Cooper, S. L. *Macromolecules* **1970**, *3*, 579.
(8) Jelinski, L. W. In *High-Resolution NMR Spectroscopy of Synthetic Polymers in Bulk*; Komoroski, R. A., Ed.; VCH Publishers: Weinheim, 1986; p 335.

(9) Spiess, H. W. *Colloid Polym. Sci.* **1984**, *261*, 193.
(10) Spiess, H. W. In *Advances in Polymer Science*; Kausch, H., Zachmann, H., Eds.; Springer Verlag: Berlin, 1984.
(11) Jelinski, L. W.; Dumais, J. J.; Engel, A. K. *Org. Coat. Appl. Polym. Sci. Proc.* **1983**, *248*, 102.
(12) Miller, J. A.; Lin, S. B.; Hwang, K. K.; Gibson, P. E.; Cooper, S. L. *Macromolecules* **1985**, *32*, 32.
(13) Eisenbach, C. D.; Baumgartner, M.; Günter, Cl. In *Advances in Elastomers and Rubber Elasticity*; Lal, J., Mark, J. E., Eds.; Plenum Publishing Corp.: New York, 1987.
(14) Camberlin, Y.; Pascault, J. P.; Letoffe, M.; Claudy, P. *J. Polym. Sci., Polym. Chem. Ed.* **1982**, *20*, 383.
(15) Yang, W. P.; Macosko, C. W.; Wellinghoff, S. T. *Polymer* **1986**, *27*, 1235.
(16) Harrell, L. L. In *Block Polymers*; Aggarwal, S. L., Ed.; Plenum Press: New York, 1970.
(17) Ng, H. N.; Allegreza, A. E.; Cooper, S. L. *Polymer* **1973**, *14*, 255.
(18) Nefzger, H. Ph.D. Thesis, Universität Karlsruhe, 1987.
(19) Eisenbach, C. D., Nefzger, H., Baumgartner, M.; Günter, Cl. *Ber. Bunsenges. Phys. Chem.* **1985**, *89*, 1190.
(20) Samuels, S. L.; Wilkes, G. L. *J. Polym. Sci., Polym. Phys. Ed.* **1973**, *11*, 807.
(21) Eisenbach, C. D.; Hayen, H.; Nefzger, H. *Makromol. Chem., Rapid Commun.* **1989**, *10*, 463.
(22) Eisenbach, C. D.; Nefzger, H. In *Multiphase Macromolecular System*; Culbertson, B., Ed.; Plenum Publishing Corp.: New York, 1989.
(23) Samuels, S. L.; Wilkes, G. L. *Polym. Lett.* **1971**, *9*, 761.
(24) Planer, G. Diploma Thesis, Universität Mainz, 1990.
(25) Enckelmann, V.; Nefzger, H.; Eisenbach, C. D., 1989, private communication; results to be published.
(26) Abragam, A. *Principles of Nuclear Magnetism*; Oxford University Press: Oxford, 1961.
(27) Pake, G. E. *J. Chem. Phys.* **1948**, *16*, 327.
(28) Hirschinger, J.; Miura, H.; Gardner, K. H.; English, A. D. *Macromolecules* **1990**, *23*, 2153. Wendoloski, J. J.; Gardner, K. H.; Hirschinger, J.; Miura, H.; English, A. D. *Science* **1990**, *247*, 431.
(29) Meltzer, A. D.; Spies, H. W.; Eisenbach, C. D.; Hayen, H. *Makromol. Chem. Rapid Commun.*, submitted for publication.
(30) Schaefer, D.; Spiess, H. W.; Suter, U. W.; Fleming, W. W. *Macromolecules* **1990**, *23*, 3431.
(31) Pschorn, U.; Rössler, E.; Sillescu, H.; Kaufmann, S.; Schaefer, D.; Spiess, H. W. *Macromolecules*, submitted for publication.
(32) Schmidt, C.; Kuhn, K. J.; Spiess, H. W. *Progr. Colloid Polym. Sci.* **1985**, *71*, 71.
(33) Polymorphism in the crystalline structure of diamine-4 has been observed (ref 22) and some hard segments may be in a glassy state.
(34) Meltzer, A. D.; Spiess, H. W.; Eisenbach, C. D.; Hayen, H. *Macromol. Notes*, submitted for publication.
(35) Meltzer, A. D.; Spiess, H. W.; Eisenbach, C. D.; Hayen, H., unpublished results.
(36) Morese-Seguela, B.; St. Jacques, M.; Renaud, J. M.; Prud'homme, J. *Macromolecules* **1980**, *13*, 100.
(37) Jelinski, L. W.; Dumais, J. J.; Engel, A. K. *Macromolecules* **1983**, *16*, 403. Jelinski, L. W.; Dumais, J. J.; Watnick, P. I.; Engel, A. K.; Sefcik, M. D. *Macromolecules* **1983**, *16*, 409. Jelinski, L. W.; Schilling, F. C.; Bovey, F. A. *Macromolecules* **1981**, *14*, 581.
(38) Froix, M. F.; Pochan, J. M. *J. Polym. Sci., Polym. Phys. Ed.* **1976**, *14*, 1047. Assink, R. A. *J. Polym. Sci., Polym. Phys. Ed.* **1977**, *15*, 59. Assink, R. A. *Macromolecules* **1978**, *11*, 1233.